¹H NMR-Based Metabolic Profiling of Urine from Mice Fed *Lentinula edodes*-Derived Polysaccharides

Xiaofei Xu, Jiguo Yang, Zhengxiang Ning, Xuewu Zhang*

College of Food Science and Engineering, South China University of Technology,
381 Wushan Road, Guangzhou 510640, China

A heteropolysaccharide, named L2, from *Lentinula edodes* has been proved to possess immunostimulating and anti-ageing activities in previous studies, but its acting mechanism was not completely understood. In this study, ¹H NMR spectroscopy approach was employed to investigate the metabolic profiles of the urine from adult mice after L2 intervention. Using principal component analysis (PCA) and partial least squares-discriminate analysis (PLS-DA), 22 potential biomarkers were found to be mainly involved in some metabolic pathways: amino acid metabolism, energy metabolism, lipid metabolism, tricarboxylic acid (TCA) cycle, urea cycle and gut microbiota metabolism. Among them, the significantly altered metabolites include: elevated glutamate (75%) and creatine (64%); decreased proline (65%), betaine (58%), fucose (63%) and dimethylamine (59%). In conclusion, the present data is helpful to understand the mechanisms related to previously confirmed immunomodulation and anti-aging effects of L2, and provide valuable information for mining new functions of L2.

INTRODUCTION

Different from other omics technologies (genomics, transcriptomics and proteomics), the metabolomics technique focuses on the changes of endogenous small molecular metabolites including amino acids, peptides, lipids, nucleic acids, organic acids, vitamins, *etc*. in biological samples [Monterio *et al.,* 2013]. It is now widely used to identify various metabolic features associated with diseases, drug treatments or diet intervention [Gibbons & Brennan, 2017]. Nuclear magnetic resonance (NMR) and mass spectrometry (MS) are the primary techniques applied in metabolomics. Compared to MS, NMR provides most reliable structural and quantitative information of metabolites, but its sensitivity is low. In contrast, MS technique has high sensitivity, but it is sometimes confusing due to the discriminated ionization ability of different types of compounds and matrix effect [Pan & Raftery, 2007]. The commonly used pattern recognition methods in the metabolomics are principal component analysis (PCA) and partial least squares-discriminate analysis (PLS-DA). PCA and PLS-DA, as an unsupervised or supervised multivariable statistical method, respectively, are able to identify metabolites that differentiate between different samples [Worley *et al.,* 2013].

Lentinula edodes is one of the most popular edible mushroom in the world. Polysaccharides are found to be one of the most important components responsible for the bioactivities of *L. edodes*. In our previous studies, a new type of heteropolysaccharide, named L2, was obtained from the fruit body of *L. edodes* with an average molecular weight of 26 KDa but without triple-helix conformation [Xu *et al.,* 2012]. *In vitro*, L2 increased the production of nitric oxide, tumor necrosis factor α, and interleukin 6 of RAW 264.7 cells in a wide range of pH circumstances with the involvement of toll-like receptor 2 [Xu *et al.,* 2012]. Further studies demonstrated that L2 still exhibited immunostimulating activity by altering the spatial structure of gut microbiota and differentially affecting gene as well as protein expressions in adult mice [Xu & Zhang, 2015; Xu *et al.,* 2015a; Xu *et al.,* 2016]. Moreover, L2 displayed anti-aging activity by restoring the age-attenuated immune responses and partly reversing the age-related composition of gut microbiota [Xu *et al.,* 2015b]. In order to better understand the acting mechanism of L2 and to further mine new functions of L2, NMR-based metabolomics approach was employed to investigate the urine metabolic profiles of the adult mice with L2 intervention.

MATERIAL AND METHODS

Animal protocols and materials

The detail processes of animal experiments were described in our previous report [Xu & Zhang, 2015]. Briefly, fourteen 8-week specific pathogen-free male C57BL/6 mice were divided into the normal group (n=7) and the L2-treated group (n=6), respectively. Gavage administration of L2 (40 mg/kg

---

body weight) to L2-treated group for 28 consecutive days was performed. Experiments were approved by the Animal Care Welfare Committee of Guangzhou University of Chinese Medicine. Adequate measurements were applied to minimize the pain of animals. 24-hour urine samples were collected on the day before euthanasia by housing the mice in metabolic cages. Samples were centrifuged at 4000 rpm for 10 min at 4°C to remove particular contaminants and then stored at -70°C for further analysis.

Preparation of sample and acquisition of ^{1}H NMR spectroscopy

Urine samples were first defrosted (one sample was contaminated and excluded in L2-treated group) and then centrifuged at $5000 \times g$ for 10 min at 4°C. The supernatant (630 µL) was transferred into 5-mm NMR tubes and then 70 µL of Anachro Certified DSS Standard Solution (ACDSS) (Anachro Technologies Inc., China) containing 5.0 mM 4,4-dimethyl-4-silapentane-1-sulfonic acid (DSS) was added according the manufacturer's instructions. All NMR spectra were recorded at 25°C on a Bruker AVANCE III-HD 600 MHz NMR spectrometer equipped with a 5mm PAQXI ^{1}H probe. ^{1}H NMR spectra were acquired using a one-dimensional NOESY (NoesyPr1d) pulse sequence (RD–90–t_1–90–t_m–90– ACQ) with water suppression during the relaxation delay of 10 s and a mixing time of 100 ms at the setting temperature of 298 K. For each urine sample, a total of 125 free induction decays (FID) were collected into 76724 data points at a flip angle of 90°, using a spectral width of 10,000 Hz, and an acquisition time of 4 s. FID was zero-filled to 64 K with an exponential function of a 0.5-Hz line-broadening factor prior to Fourier transformation.

Data pre-processing of NMR spectra and multivariate statistical analysis

All NMR spectra were phased, corrected for baseline distortion, referenced to the methyl group of DSS at δ 0.000 and carefully aligned using the software of MestReNova 10.0.2 (Mestrelab Research S.L, Santiago de Compostela, Spain). The regions corresponding to residual water and urea, and DSS (4.5–6, and 0.0–0.5 ppm, respectively) were excluded in all spectra. The remaining regions of spectra were segmented into 0.01 ppm bins. The resulting integrals were then normalized to the total of the spectral area to partially compensate for differences in the concentrations of samples and converted to ASCII format. For metabolites identification, NMR spectral data analysis was accomplished using targeted profiling with Chenomx NMR Suite 4.6 (Chenomx Inc, Canada), which compares a known reference signal (DSS) with signals derived from a library of compounds containing chemical shifts and peak multiplicities and human metabolome database [HMDB]. The biofunction information of the identified metabolites were derived from HMDB (http://www.hmdb.ca/).

Subsequently, the NMR spectral data were imported into SIMCA-P 12.0 software (Umetrics, Umeå, Sweden) for analysis and visualization by multivariate statistical methods. Data was mean-centered and Pareto-scaled to avoid NMR measurement noise prior to principal component analysis (PCA)

and partial least squares discriminant analysis (PLS-DA) [Xu *et al*., 2015]. The quality of the models obtained from PCA (only R^2X(cum) and Q^2(cum) were extracted from PCA model) and PLS-DA was determined by R^2X(cum) and Q^2(cum) values, which indicate the goodness of fit parameter (R^2X) and the predictive ability parameter (Q^2) of the model, respectively. The reliability of the model increases with R^2X and Q^2 approaching 1. The values of $Q^2 \geq 0.5$ indicate the good quality of the model. Due to the small number of samples, the seven-round cross validation were performed to assess the robustness of the model.

Quantitative statistical analysis

Quantitative comparison of metabolites based on signal intensity in urine samples was done using a non-parametric one-way analysis of variance (Mann-Whitney test). The metabolites with high VIP (variable importance in projection) value in each PLS-DA model were selected for further analysis in two groups. Those variables with VIP value >1.0 and p<0.05 were considered as potential biomarkers. The potential biomarkers were further analyzed using integrating enrichment analysis and pathway topology analysis and visualization with MetaboAnalyst 3.0 (http://www.metaboanalyst.ca) [Xia *et al.*, 2015]. Statistical significance was considered at p<0.05. Statistical analyses were performed with SPSS 11.5.

RESULTS

^{1}H-NMR based metabolomics analysis

Metabolites in urine samples from normal and L2-treated group mice were profiled by ^{1}H-NMR and typical spectra of different samples were given in Figure 1. A total of 35 compounds have been identified, which include: (1) amino acids: leucine, isoleucine, valine, proline, methionine, lysine, glycine, N-acetylglutamic acid, *etc*.; (2) organic acids: lactate, propionate, citrate, malate, 2-oxoglutarate, succinate, *etc*.; (3) energy metabolites: creatine, creatinine, adenosine, *etc*.; (4) intestinal bacteria-metabolized products: dimethylamine(DMA), trimethylamine (TMA), phenylacetylglulamine, phenylacetylglycine, trimethylamine oxide (TMAO), hippurate, *etc*.; and (5) others: choline, glucose, fucose, *etc.*

Effect of L2 on urine metabolic profiling

In order to compare metabolic profiling between normal and treatment groups, the unsupervised PCA analysis was firstly used to visualize general clustering trends among the observations, and also to know whether the two groups could be distinguished based on their metabolic profiling provided by NMR. The PCA scores plot (Figure 2) showed that the separation between normal and treatment groups was not obvious. The first two principal components accounted for 29.8% and 17.7% of the variance in NMR data, respectively. The parameters ($R^2X=0.474$, $Q^2=0.0824$, $Q^2<0.5$) indicated low predictability for PCA model.

After PCA, supervised PLS-DA was applied to evaluate the systemic changes in the metabolomics of L2-treated mice, a PLS-DA model was established based on the data of normal
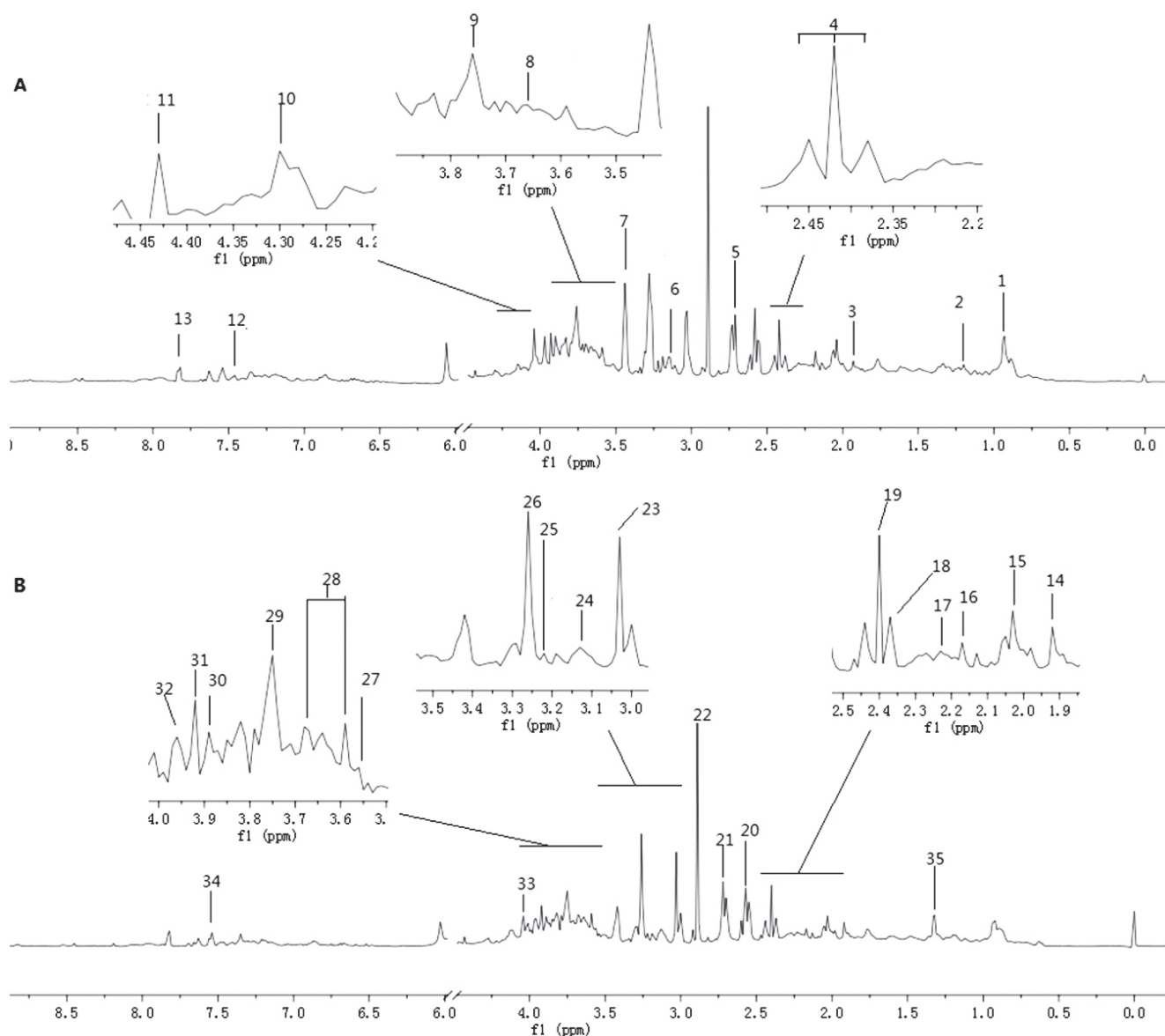
FIGURE 1. Representative 600 MHz ^{1}H NMR spectra of urinary samples obtained from normal mouse (A) and L2-treated mouse (B). Key for spectra: 1, isoleucine; 2, fucose; 3, arginine;4, 2-oxoglutarate;5, dimethylamine;6, citrulline; 7, proline; 8, phenylacetylglutamine; 9, leucine;10, adenosine; 11, trigonelline; 12, niacin; 13, benzoate; 14, lysine; 15, N-acetylglutamic acid; 16, propionate; 17, valine; 18, glutamate; 19, succinate; 20, citrate; 21, malate; 22, trimethylamine; 23, creatinine;24, malonic acid; 25, betaine; 26, trimethylamine oxide (TMAO); 27, glycine; 28, glucose; 29, phenylacetyl-glycine; 30, methionine; 31, creatine;32, phenylalanine; 33, choline; 34, hippurate; 35, lactate.

and treatment groups. As shown in the scores plot (Figure 3), the two groups were clearly discriminated, which implied that mice from normal and L2 treatment had distinct urine metabolomic characteristics. The quality parameters of the PLS--DA model ($R^2X=0.506$ and $Q^2=0.663$, $Q^2>0.5$) indicated that good separation of different groups was achieved, suggesting that biochemical changes happened in the urine of L2 treated group, and a reliable PLS-DA model was established. To visualize the importance of variables to the classification, those variables with VIP values >1 were the mainly contributing metabolites and were shown in the loading plot (Figure 4). The farther to the origin, the greater the contribution to the classification in the loading plot.

Identification of potential biomarkers for L2 intervention

The changed metabolites, p-value below 0.05, were considered as candidate potential biomarkers. Based on this, 22 differential metabolites between normal and L2 treatment groups were identified in urine samples (Table 1), which were considered as potential biomarkers that correlated with how L2 influenced the physiological metabolism of adult mice. The VIP values of all the candidate metabolites in PLS-DA model were employed to determine their contribution to group separation. The altered metabolites with VIP value >1 in L2 treatment (Table 1) were mainly involved in amino acids (significantly ($p<0.05$) increased levels of leucine, isoleucine, glutamate, glycine and phenylalanine,
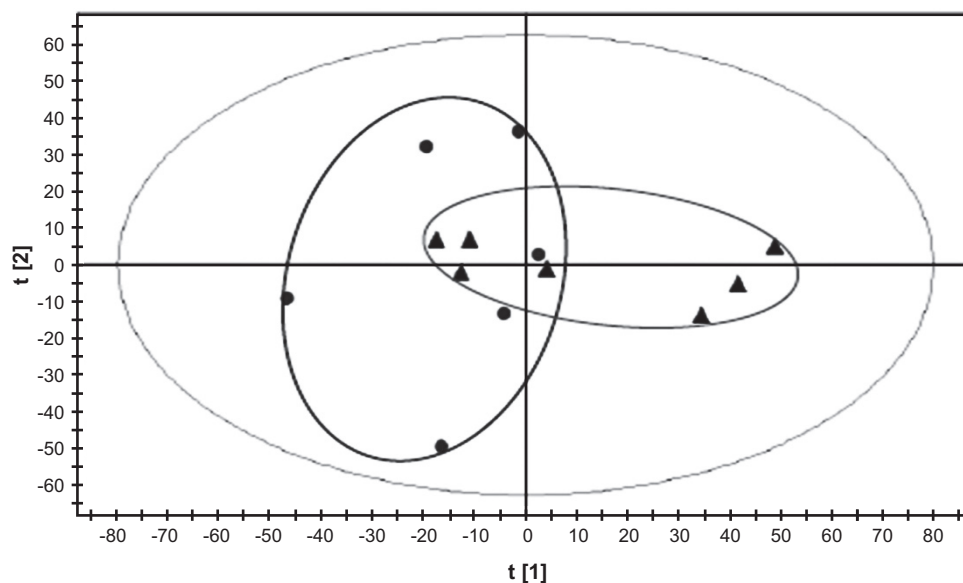
FIGURE 2. PCA score plot based on ¹H NMR spectral data of urine samples from normal mice (black triangle , n=7) and L2-treated mice (black circle, n=6).
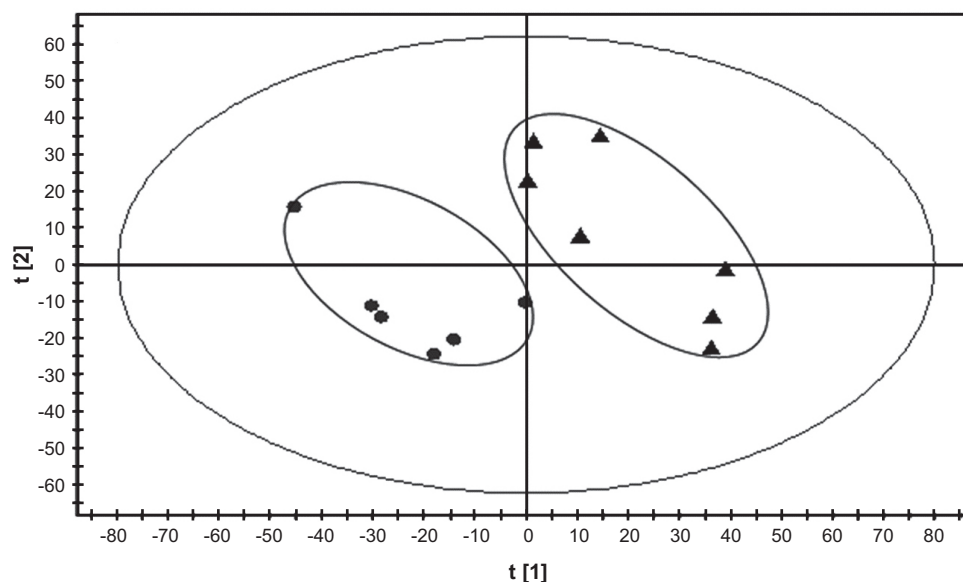

FIGURE 3. PLS-DA score plot based on ¹H NMR metabolomics data for normal group (black triangle, n=7) and L2-treated group (black circle, n=6).

but significantly ($p<0.01$) decreased in proline, and citrulline ($p<0.05$)), metabolic products related to gut microbiota (increased in phenylacetylglutamine and phenylacetylglycine ($p<0.05$), but decreased in DMA, tartrate and benzonate ($p<0.05$)), organic acids (decreased in 2-oxoglutarate, malonic acid, and malate ($p<0.05$)), energy metabolism (increased in glucose and creatine ($p<0.05$), but decreased creatinine, trigonelline and niacin ($p<0.05$)), and phospholipids metabolism (decreased in betaine ($p<0.05$) as well as glycan and glycolipid metabolism (decreased in fucose ($p<0.05$)).

Perturbed metabolic pathway analysis

Based on the significantly altered metabolite markers, more detailed analysis of pathways and networks regulated by L2 were performed using MetaboAnalyst data annotation approach. The multi-pathway metabolic perturbation associated with L2 treatment was summarized in Table 2. Top 3 metabolic pathways of importance included amino acids synthesis and metabolism (glutamine and glutamate metabolism, glycine, serine and threonine metabolism, phenylalanine metabolism, phenylalanine, tyrosine and tryptophan biosynthesis), aminoacyl-tRNA biosynthesis (Raw $p<0.05$), and gut microbiota-related metabolism because five identified metabolites including DMA, phenylacetylglutamine, phenylacetyglycine, tartrate, and benzoate were co-metabolites of the host and gut microbiota (notably, the gut microbiota-related metabolites not available in the database of MetaboAnalyst 3.0).
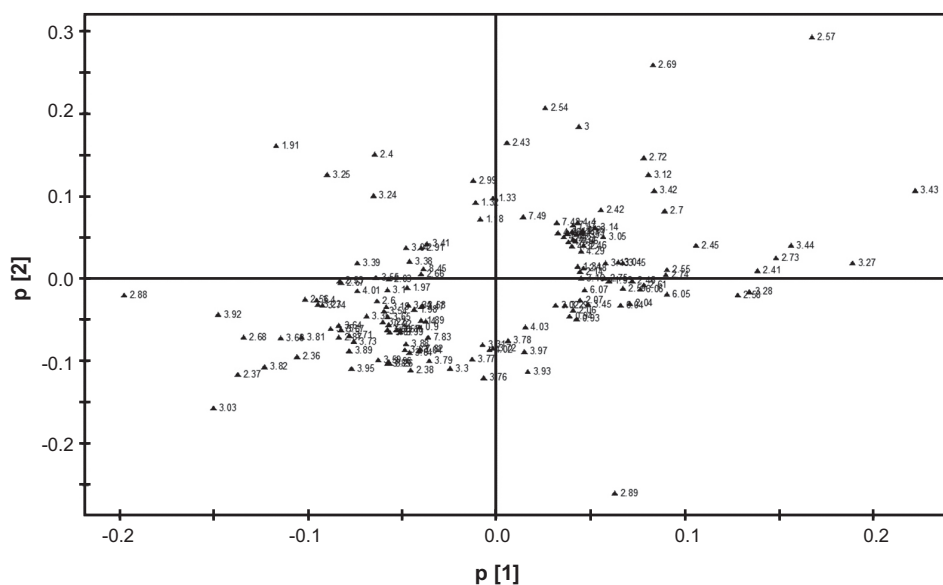
FIGURE 4. PLS-DA loading plot based on ¹H NMR metabolomics data. Spots representing variables with VIP values >1 are shown.

DISCUSSION

Currently, not too much studies are available on the application of metabolomics method to the intervention effect and metabolism regulations of polysaccharides, especially for mushroom polysaccharides. For example, using biochemical parameters coupled with metabolomics based on gas chromatography–mass spectrometry (GC–MS), Ji *et al.* [2014] investigated the hepatoprotective effect of *Angelica sinensis* polysaccharides; employing an MS-based metabolomics approach, Wang *et al.* [2015] analyzed the serum and hepatic metabolic profiles of the mice with ethanol-induced liver injury and oral administration of *Dendrobium huoshanense* polysaccharide; while based on ultra-performance liquid chromatography quadrupole time-of-flight mass spectrometry (UPLC-Q-TOF/MS), Zhu *et al.* [2016] explored the effect of *Ganoderma atrum*-derived polysaccharide on the serum metabolites of type 2 diabetic rats. In this study, urine metabolomics profiling was performed by NMR; the results revealed that *L. edodes*-derived polysaccharide L2 exposure dramatically altered a number of metabolic pathways including amino acid metabolism, tricarboxylic acid (TCA)/urea cycles, energy/lipid metabolism and gut microbiota-involved metabolism.

For amino acid metabolism, the relative concentrations of two branched chain amino acids (BCAAs) (leucine and isoleucine), glycine and phenylalanine were increased by 13–22%, in particular, 65% of reduction in proline and 75% of elevation in glutamate were observed in L2 treatment group in contrast to normal group. It was reported that BCAAs supplementation improved intestinal immune defense function by increasing intestinal immunoglobulins in weaned piglets [Ren *et al.,* 2015]. BCAAs were also discovered to extend the life span of yeast [Alvers *et al.,* 2009] and increase the average life span of male mice [D'Antona *et al.,* 2010], suggesting that BCAA may play a role in aging process. Studies observed that the increases in BCAA were associated with

anti-hyperlipidemia effect of a traditional Chinese medicine Xu-Fu-Zhu-Yu in rats [Song *et al.,* 2013], and the intervention of curcumin on hyperlipidemia mice also led to elevated levels of BCAA [Li *et al.*, 2015]. Recently, the levels of BCAAs in serum were found to be associated with the gut bacterial species of *Prevotella copri* and *Bacteroides vulgatus* [Pedersen *et al.*, 2016]. In particular, *P. copri* alone can increase the circulating levels of BCAAs in mice [Pedersen et al., 2016]. L2 exhibited altering the gut bacterial groups related to *Prevotellaceae* and *Bacteroidaceae* in mice [Xu & Zhang, 2015], suggesting that the changed levels of BCAAs in the present study may be partially attributed to the alteration of gut microbiota composition. In addition, high serum phenylalanine concentration was found to be related to immune activation in patients with Alzheimer's disease [Wissmann *et al.*, 2013]. Glycine administration was confirmed to avoid the characteristic immunodeficiencies in the experimentally diabetic rats [Lezcano Meza *et al.,* 2006]. Proline was reported to be correlated to the degree of alcoholic liver injury [Lieber, 2000]. Previous study demonstrated that glutamate can amplify insulin release after its uptake into insulin granules mediated by cAMP/PKA signaling [Gheni *et al.*, 2014]. Glutamate production is diminished in animal models of human diabetes and obesity, whereas in these models insulin secretion can be restored by a membrane-permeable glutamate precursor. In the present study, L2 remarkably increased the production of glutamate, suggesting potential of L2 in amplifying insulin secretion. Except amino acid transamination, glutamate is involved in a number of key functions in lymphocytes, macrophages and neutrophils. Glutamate is required as a precursor for ornithine synthesis in macrophages and monocytes. This pathway is linked to the urea cycle and ultimately results in formation of arginine, a substrate for inducible nitric oxide synthase. Glutamate may also serve as a precursor for glutathione synthesis, which may play a direct role in antioxidant defenses [Gleeson & Bishop, 2000]. Hence, based on the intervention effects of L2 on amino acids metabolism, it is pos-

TABLE 1. Identification of urinary metabolites with VIP value>1 selected as potential biomarkers and their change trends.

No.	Metabolites	VIP	Metabolic change	Chemical moiety	δ^1H(ppm)	Biofunction
1	Isoleucine	1.49	↑*	α-CH, β-CH,γ-CH₃, one of γ-CH₂, one of γ-CH₂, δ-CH₃	3.65(d), 1.98(m), **0.99(d)**, 1.40(m), 1.20(m), 0.92(t)	Component of BCAA biosynthesis. Particular involvement in stress, energy and muscle metabolism.
2	Proline	5.52	↓**	α-CH, one of β-CH₂, one of β-CH₂, one of β-CH₂, one of δ-CH₂, half δ-CH₂, γ-CH₂	4.13(dd), **3.44(s)**, 3.34(m), 2.35(m), 2.06(m), 2.05(m), 2.01(m)	Component of arginine and proline metabolism.
3	Glutamate	3.51	↑**	α-CH, β-CH₂, γ-CH₂	2.11(m), **2.37(m)**, 3.78(m)	A key molecule in cellular metabolism as component of amino biosynthesis and metabolism.
4	2-oxoglutarate	2.64	↓*	β-CH₂, γ-CH₂	**2.44(t)**, 3.01(t)	A key intermediate in the TCA cycle. Component of amino acid biosynthesis and metabolism.
5	Dimethylamine	3.73	↓*	2×CH₃	**2.73(s)**	Co-metabolites by gut microbiota and host.
6	Creatinine	1.45	↓**	CH₂, NCH₃,	4.06(s), **3.05(s)**	A breakdown product of creatine phosphate in muscle. The most commonly used indicator of renal function.
7	Malonic acid	2.39	↓*	CH₂	**3.13(s)**	A competitive inhibitor of the enzyme succinate dehydrogenase in the respiratory electron transport chain.
8	Betaine	4.79	↓*	CH₂, CH₃	**3.27(s)**, 3.94(s)	Function as a methyl donor which is important to proper liver function, cellular replication, and detoxification reactions.
9	Citrulline	1.67	↓*	CH, CH₂	3.75(dd), **3.15(q)**	Intermediate product of the urea cycle.
10	Fucose	3.91	↓*	CH₃, 1-CH, 2-CH, 3-CH, 4-CH, 5-CH, 6-CH	1.20(d), **1.24(d)**, 3.43(dd), 3.63(dd), 3.74(m), 3.85(dd), 4.18(q)	A common component of N- and O-linked glycans and glycolipids produced by mammalian cells.
11	Glucose	2.60	↑*	1-CH, 2-CH, 3-CH, 4-CH, 5-CH, one of 6-CH₂, one of 6-CH₂	5.23(d), **3.59(dd)**, 3.71(t), **3.64(m)**, 3.81(m), 3.73(dd), 3.89(m)	A primary source of energy for living organisms.
12	Glycine	1.50	↑**	CH₂	**3.54(s)**	Involved in the synthesis of DNA, phospholipids and collagen, and in release of energy.
13	Phenylacetylglulamine	1.53	↑*	CH	**3.66(q)**	A major nitrogenous co-metabolite by gut microbiota and host
14	Leucine	1.98	↑**	α-CH, β-CH₂, γ-CH, δ-CH₃, δ-CH₃	**3.75(m)**, 1.67(m), 1,73(m), 0.95(d), 0.98(d)	Component of BCAA biosynthesis. Particular involvement in stress, energy and muscle metabolism.
15	Phenylacetylglycine	2.21	↑*	2,6-CH, 3,5-CH, 7-CH, 10-CH	7.40(m), 7.34(m), **3.74(d)**, 3.65(s)	A co-metabolite by gut microbiota and host.
16	Creatine	3.69	↑*	CH₃, CH₂	3.02(s), **3.92(s)**	Function as part of the cell's energy shuttle.
17	Phenylalanine	1.41	↑*	2,6-CH, 3,5-CH, 4-CH, one of β-CH₂, one of β-CH₂, α-CH	7.40(m), 7.35(m), 7.30(m), 3.13(dd), 3.28(dd), **3.95(m)**	Component of amino acid biosynthesis and metabolism.
18	Malate	1.02	↓*	α-CH, β-CH₂	**2.68(dd)**, 2.36(dd)	An intermediate of the TCA cycle. Component of Pyruvate metabolism.
19	Tartrate	1.11	↓**	CH	4.34(s)	Metabolites of gut microbiota after food consumption.
20	Trigonelline	1.29	↓**	2-CH, 4-CH, 6-CH, 5-CH, CH₃	4.40(s), **4.44(s)**	A product of the metabolism of niacin.
21	Niacin	1.10	↓**	CH, CH	**7.48(d)**	Essential in energy metabolism in the living cell and DNA repair.
22	Benzoate	1.18	↓**	2,6-CH, 3,5-CH, 4-CH	7.46(dd), 7.54(t), **7.86(d)**	A co-metabolite by gut microbiota and host.

Note: s, singlet; d, doublet; t, triplet; q, quartet; m, other multiplet; dd, doublet of doublets. Bold letters indicated these peaks were visually assigned in Figure 1. The arrows demonstrate that the metabolic change is significantly increased (↑) or decreased (↓) in L2-treated mice compared to normal mice. The *p* values were analyzed using Mann-Whitney test based on the integrals of the selected peaks. *$p<0.05$, **$p<0.01$. Biofunction information derived from HMDB database. TCA, tricarboxylic acid. BCAA, branched chain amino acid.

TABLE 2. Enrichment pathway analysis for potential markers of L2-treatment.

No.	Metabolic pathway	Total	Hits	Raw p
1	Glutamine and glutamate metabolism	5	2	0.0018461
2	Glycine, serine and threonine metabolism	31	3	0.0084051
3	Phenylalanine metabolism	11	2	0.0096493
4	Aminoacyl-tRNA biosynthesis	69	4	0.013812
5	Arginine and proline metabolism	44	3	0.022021
6	Phenylalanine, tyrosine and tryptophan biosynthesis	4	1	0.055331
7	Cyanoamino acid metabolism	6	1	0.081893
8	Methane metabolism	9	1	0.12041
9	Nitrogen metabolism	9	1	0.12041
10	Valine, leucine and isoleucine biosynthesis	11	1	0.14523
11	Nicotinate and nicotinamide metabolism	13	1	0.16938
12	Starch and sucrose metabolism	19	1	0.23801
13	Citrate cycle (TCA cycle)	20	1	0.24891
14	Fructose and mannose metabolism	21	1	0.25967
15	Butanoate metabolism	22	1	0.27027
16	Alanine, aspartate and glutamate metabolism	24	1	0.29105
17	Glutathione metabolism	26	1	0.31127
18	Galactose metabolism	26	1	0.31127
19	Porphyrin and chlorophyll metabolism	27	1	0.32118
20	Amino sugar and nucleotide sugar metabolism	37	1	0.41304
21	Valine, leucine and isoleucine degradation	38	1	0.42155
22	Primary bile acid biosynthesis	46	1	0.48551

The Total is the total number of compounds in the metabolic pathway; the Hits is the actually matched number from the identified data; the Raw p is the original p value calculated from the enrichment analysis by MetaboAnalyst 3.0.

sible that L2 could have potential benefits to immune function, anti-aging, anti-hyperlipidemia, ethanol-induced liver injury protection, insulin resistance improvement and antioxidant defense by altering the above amino acids metabolism.

As a member of TCA cycle, the relative level of 2-oxoglutarate was decreased by 41% in response to L2 treatment. It was reported that the reduction of 2-oxoglutarate could be related to antioxidant activity, for it was depleted by scavenging hydrogen peroxide and converted to succinate [Long & Halliwell, 2011]. A recent study indicated that 2-oxoglutarate acted as a metabolic regulator of CD4(+) T cell differentiation by entering into the mitochondrial citric acid cycle [Klysz et al., 2015]. A decrease in the intracellular amount of 2-oxoglutarate shifted the balance between the generation of type 1 helper T cells and T regulatory (Treg) cells toward

that of a Treg phenotype. Thus, there is a link between reduction of 2-oxoglutarate and immunomodulation.

For energy metabolism, the relative levels of creatinine, trigonelline and malonic acid were reduced by 25%, 31% and 38%, respectively, while the relative level of creatine was increased by 64%, in L2-treated group. Creatine has potential benefits in aging populations, such as, lifespan extension [Ferrante et al., 2000], slowing down the progression of Parkinson's disease [NINDS NET-PD Investigators, 2006], memory improvement [McMorris et al., 2007], and stroke prevention [Perasso et al., 2013].

In lipid metabolism pathway, the relative concentration of betaine was greatly decreased by 58% in L2-treated mice. In cells with vitamin B-6 deficiency, >200% high concentration of betaine was observed [da Silva et al., 2014]. Manna et al. [2014] indicated that betaine was elevated in tumor tissue and urine from colorectal tumor-bearing mice. Ascha et al. [2016] showed a significantly high level of betaine in patients with alcoholic hepatitis (AH). Obi et al. [2016] reported that betaine was increased in aged venous thrombosis mice compared with young animals.

As the initial metabolite of the urea cycle, the relative level of citrulline was decreased by 26% after L2 treatment. It was reported that the level of citrulline was abundant in the elderly, suggesting an impaired urea cycle [Chaleckis et al., 2016]. Schoeman et al. [2016] pointed out that the progression of chronic hepatitis B virus (HBV) was associated with increased concentration of citrulline, reflective of a dysregulated urea cycle in the HBV envelope antigen-negative phase.

In response to L2 intervention, the relative concentration of two monosaccharides was remarkably changed: fucose was reduced by 63%, but glucose was increased by 43%. Fucose was reported to be associated with intestinal inflammation in a mouse model of Crohn's disease [Lin et al., 2010]. It is well established that glucose was of great importance in macrophage metabolism and activation [Bordbar et al., 2012]. High glucose concentration of LPS-stimulated macrophages was shown to increase NO production [de Souza et al., 2008]. Jung et al. [2013] reported that sera of asthma patients were characterized by decreased levels of glucose. Hence, the decreased fucose and the increased glucose could be helpful to inflammation, immune activation, and asthma.

In gut microbiota-involved metabolism, 5 metabolites were perturbed: the relative levels of phenylacetylglulamine and phenylacetylglycine were increased by 13% and 15%, respectively; while tartrate, benzoate and dimethylamine (DMA) were decreased by 25%, 31% and 59%, respectively. Using a targeted metabolomics analysis, phenylacetylglutamine was identified as a key gut microbiota-host co-metabolite in rat [Hou et al., 2016]. By analyzing metabolite association with 16S gut microbiome profiles, Barrios et al. [2015] found that 52 Operational Taxonomic Units (OTUs) were significantly associated with phenylacetylglutamine, and these microbial members belong to the order Clostridiales. Phenylacetylglutamine was considered to be a metabolic signature of extreme longevity in northern Italian centenarians: the increased excretion of phenylacetylglutamine in urine of centenarians [Collino et al., 2013]. As a gut microbial co-metabolites [Yap et al., 2008], the concentration of phenyl-
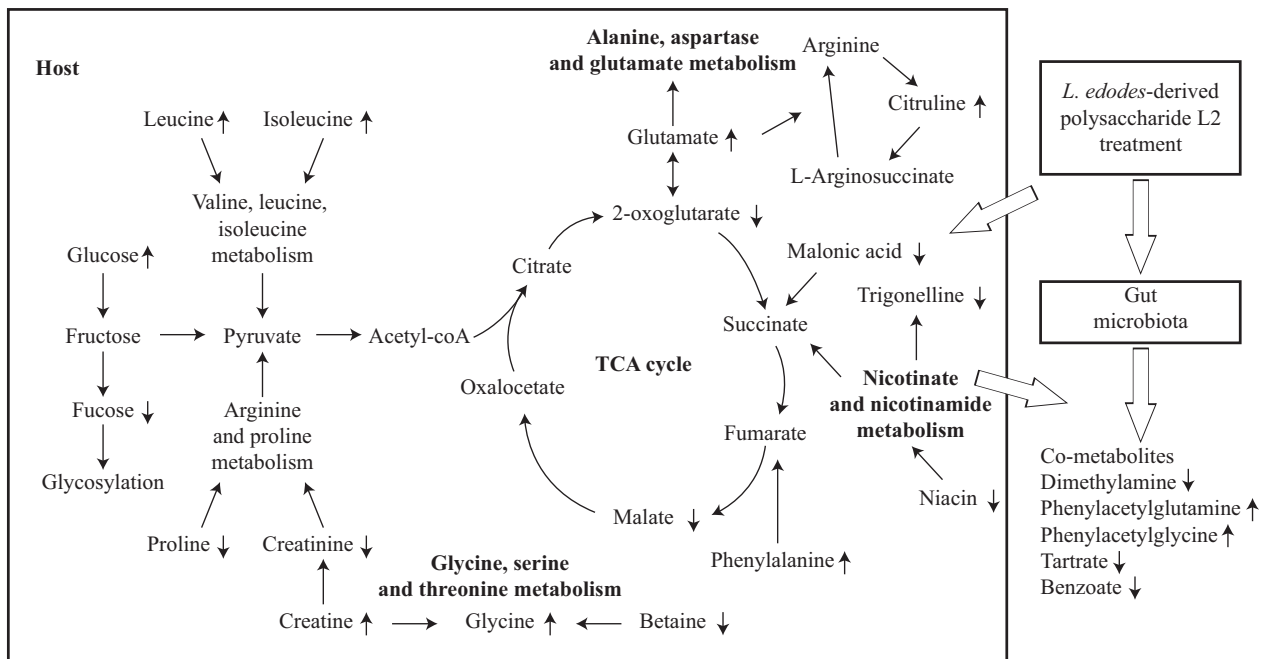
FIGURE 5. Potential pathways perturbed by *L. edodes*-derived polysaccharide L2 in adult mice based on KEGG pathway. The ↑ or ↓ was an indicator of changed metabolites in urine as compared with the normal mice.

acetylglycine was increased in the urine metabolome of rats treated with N-carbamylglutamate (a compound for oxidative stress treatment) [Liu *et al.*, 2016]. Previous study showed that the metabolites: dimethylamine (DMA), trimethylamine (TMA), and trimethylamine oxide (TMAO), are derived only from symbiotic bacterial metabolism and not from mammalian metabolism in mice, for germ-free mice do not excrete TMA [al-Waiz *et al.*, 1992]. Richards *et al.* [2013] indicated that an aging metabolic phenotype independent of diet was characterized by high levels of methylamine, DMA, TMAO and other metabolites in a lifelong dog, thus, the reduction of these metabolites could be helpful for anti-aging. Wu *et al.* [2008] found that many metabolites like DMA and TMAO were reset to younger levels in the rats, which was one potential mechanism for the anti-aging effects of the total flavone of *Epimedium*. These results suggest potential benefits of L2 to oxidative stress treatment and anti-ageing by the altered microbiota-derived metabolites.

CONCLUSIONS

NMR-based metabolomics approach was successfully employed to analyze the alterations in the metabolic profiles of urine from adult mice treated with *L. edodes*-derived polysaccharide L2. Twenty two potential biomarkers were identified, which were involved in a number of metabolic pathways: amino acids metabolism, energy metabolism, lipid metabolism, TCA cycle, urea cycle, glycolysis, gut microbiota metabolism, *etc*. The potential metabolic pathways or networks were structured in Figure 5. The differentially changed metabolites can help to understand the acting mechanisms related to previously confirmed immunomodulation and anti-aging activities of L2, and provide valuable information for mining new functions of L2.

CONFLICT OF INTERESTS

The authors report no declarations of interest.

REERENCES

1. Alvers A.L., Fishwick L.K., Wood M.S., Hu D., Chung H.S., Dunn W.A. Jr., Aris J.P., Autophagy and amino acid homeostasis are required for chronological longevity in *Saccharomyces cerevisiae*. Aging Cell, 2009, 8(4), 353–369.

2. Al-Waiz M., Mikov M., Mitchell S.C., Smith R.L., The exogenous origin of trimethylamine in the mouse. Metabolism, 1992, 41(2), 135–136.

3. Ascha M., Wang Z., Ascha M.S., Dweik R., Zein N.N., Grove D., Brown J.M., Marshall S., Lopez R., Hanouneh I.A., Metabolomics studies identify novel diagnostic and prognostic indicators in patients with alcoholic hepatitis. World J. Hepatol., 2016, 8(10), 499–508.

4. Barrios C., Beaumont M., Pallister T., Villar J., Goodrich J.K., Clark A., Pascual J., Ley R.E., Spector T.D., Bell J.T., Menni C., Gut-microbiota-metabolite axis in early renal function decline. PLoS One, 2015, 10(8), art. no. e0134311.

5. Bordbar A., Mo M.L., Nakayasu E.S., Schrimpe-Rutledge A.C., Kim Y.M., Metz T.O., Jones M.B., Frank B.C., Smith R.D., Peterson S.N., Hyduke D.R., Adkins J.N., Palsson B.O., Model-driven multi-omic data analysis elucidates metabolic immunomodulators of macrophage activation. Mol. Syst. Biol., 2012, 8, art. no. 558.

6. Chaleckis R., Murakami I., Takada J., Kondoh H., Yanagida M., Individual variability in human blood metabolites identifies age-related differences. Proc. Natl. Acad. Sci. USA, 2016, 113(16), 4252–4259.

7. Collino S., Montoliu I., Martin F.P., Scherer M., Mari D., Salvioli S., Bucci L., Ostan R., Monti D., Biagi E., Brigidi P., Franceschi C., Rezzi S., Metabolic signatures of extreme longevity in northern Italian centenarians reveal a complex remodeling of lipids, amino acids, and gut microbiota metabolism. PLoS One, 2013, 8(3), art. no. e56564.

8. da Silva V.R., Ralat M.A., Quinlivan E.P., DeRatt B.N., Garrett T.J., Chi Y.Y., Frederik Nijhout H., Reed M.C., Gregory J.F., Targeted metabolomics and mathematical modeling demonstrate that vitamin B-6 restriction alters one-carbon metabolism in cultured HepG2 cells. Am. J. Physiol. Endocrinol. Metab., 2014, 307(1), E93–101.

9. D'Antona G., Ragni M., Cardile A., Tedesco L., Dossena M., Bruttini F., Caliaro F., Corsetti G., Bottinelli R., Carruba M.O., Valerio A., Nisoli E., Branched-chain amino acid supplementation promotes survival and supports cardiac and skeletal muscle mitochondrial biogenesis in middle-aged mice. Cell Metab., 2010, 12(4), 362–372.

10. de Souza L.F., Jardim F.R., Sauter I.P., de Souza M.M., Bernard E.A., High glucose increases RAW 264.7 macrophages activation by lipoteichoic acid from *Staphylococcus aureus*. Clin. Chim. Acta., 2008, 398(1–2), 130–133.

11. Ferrante R.J., Andreassen O.A., Jenkins B.G., Dedeoglu A., Kuemmerle S., Kubilus J.K., Kaddurah-Daouk R., Hersch S.M., Beal M.F., Neuroprotective effects of creatine in a transgenic mouse model of Huntington's disease. J. Neurosci., 2000, 20(12), 4389––4397.

12. Gheni G., Ogura M., Iwasaki M., Yokoi N., Minami K., Nakayama Y., Harada K., Hastoy B., Wu X., Takahashi H., Kimura K., Matsubara T., Hoshikawa R., Hatano N., Sugawara K., Shibasaki T., Inagaki N., Bamba T., Mizoguchi A., Fukusaki E., Rorsman P., Seino S., Glutamate acts as a key signal linking glucose metabolism to incretin/cAMP action to amplify insulin secretion. Cell Rep., 2014, 9(2), 661–673.

13. Gibbons H., Brennan L., Metabolomics as a tool in the identification of dietary biomarkers. Proc. Nutr. Soc., 2017, 76(1), 42–53.

14. Gleeson M., Bishop N.C., Modification of immune responses to exercise by carbohydrate, glutamine and anti-oxidant supplements. Immunol. Cell Biol., 2000, 78, 554–561.

15. Hou W., Zhong D., Zhang P., Li Y., Lin M., Liu G., Yao M., Liao Q., Xie Z., A strategy for the targeted metabolomics analysis of 11 gut microbiota-host co-metabolites in rat serum, urine and feces by ultra-high performance liquid chromatography-tandem mass spectrometry. J. Chromatogr. A., 2016, 1429, 207–217.

16. Ji P., Wei Y., Sun H., Xue W., Hua Y., Li P., Zhang W., Zhang L., Zhao H., Li J., Metabolomics research on the hepatoprotective effect of Angelica sinensis polysaccharides through gas chromatography-mass spectrometry. J Chromatogr. B Analyt. Technol. Biomed. Life Sci., 2014, 973, 45–54.

17. Jung J., Kim S.H., Lee H.S., Choi G.S., Jung Y.S., Ryu D.H., Park H.S., Hwang G.S., Serum metabolomics reveals pathways and biomarkers associated with asthma pathogenesis. Clin. Exp. Allergy, 2013, 43(4), 425–433.

18. Klysz D., Tai X., Robert P.A., Craveiro M., Cretenet G., Oburoglu L., Mongellaz C., Floess S., Fritz V., Matias M.I., Yong C., Surh N., Marie J.C., Huehn J., Zimmermann V., Kinet S., Dardalhon V., Taylor N., Glutamine-dependent α-ketoglutarate production regulates the balance between T helper 1 cell and regulatory T cell generation. Sci. Signal., 2015, 8(396), ra97.

19. Lezcano Meza D., Terán Ortiz L., Carvajal Sandoval G., Gutiérrez de la Cadena M., Terán Escandón D., Estrada Parra S., Effect of glycine on the immune response of the experimentally diabetic rats. Rev. Alerg. Mex., 2006, 53(6), 212–216.

20. Li Z.Y., Ding L.L., Li J.M., Xu B.L., Yang L., Bi K.S, Wang Z.T., H-1-NMR and MS based metabolomics study of the intervention effect of curcumin on hyperlipidemia mice induced by high-fat diet. PLoS One, 2015, 10, art. no. e0120950.

21. Lieber C.S., Alcoholic liver disease: new insights in pathogenesis lead to new treatments. J. Hepatol., 2000, 32(1 Suppl), 113–128.

22. Lin H.M., Barnett M.P., Roy N.C., Joyce N.I., Zhu S., Armstrong K., Helsby N.A., Ferguson L.R., Rowan D.D., Metabolomic analysis identifies inflammatory and noninflammatory metabolic effects of genetic modification in a mouse model of Crohn's disease. J. Proteome Res., 2010, 9(4), 1965–1975.

23. Liu G., Xiao L., Cao W., Fang T., Jia G., Chen X., Zhao H., Wu C., Wang J., Changes in the metabolome of rats after exposure to arginine and N-carbamylglutamate in combination with diquat, a compound that causes oxidative stress, assessed by ^{1}H NMR spectroscopy. Food Funct., 2016, 7(2), 964–974.

24. Long L.H., Halliwell B., Artefacts in cell culture: α-Ketoglutarate can scavenge hydrogen peroxide generated by ascorbate and epigallocatechin gallate in cell culture media. Biochem. Biophys. Res. Commun., 2011, 406(1), 20–24.

25. Manna S.K., Tanaka N., Krausz K.W., Haznadar M., Xue X., Matsubara T., Bowman E.D., Fearon E.R., Harris C.C., Shah Y.M., Gonzalez F.J., Biomarkers of coordinate metabolic reprogramming in colorectal tumors in mice and humans. Gastroenterology, 2014, 146(5), 1313–1324.

26. McMorris T., Mielcarz G., Harris R.C., Swain J.P., Howard A., Creatine supplementation and cognitive performance in elderly individuals. Neuropsychol. Dev. Cogn. B Aging Neuropsychol. Cogn., 2007, 14(5), 517–528.

27. Monteiro M.S., Carvalho M., Bastos M.L., Guedes de Pinho P., Metabolomics analysis for biomarker discovery: advances and challenges. Curr. Med. Chem., 2013, 20(2), 257–271.

28. NINDS NET-PD Investigators., A randomized, double-blind, futility clinical trial of creatine and minocycline in early Parkinson disease. Neurology, 2006, 66(5), 664–671.

29. Obi A.T., Stringer K.A., Diaz J.A., Finkel M.A., Farris D.M., Yeomans L., Wakefield T., Myers D.D. Jr., 1D-(1)H-nuclear magnetic resonance metabolomics reveals age-related changes in metabolites associated with experimental venous thrombosis. J. Vasc. Surg. Venous Lymphat. Disord., 2016, 4(2), 221–230.

30. Pan Z., Raftery D., Comparing and combining NMR spectroscopy and mass spectrometry in metabolomics. Anal. Bioanal. Chem., 2007, 387, 525–527.

31. Pedersen H.K., Gudmundsdottir V., Nielsen H.B., Hyotylainen T., Nielsen T., Jensen B.A.H., Forslund K., Hildebrand F., Prifti E., Falony G., Le Chatelier E., Levenez F., Doré J., Mattila I., Plichta D.R., Pöhö P., Hellgren L.I., Arumugam M., Sunagawa S., Vieira-Silva S., Jørgensen T., Holm J.B., Trošt K., Consortium

M., Kristiansen K., Brix S., Raes J., Wang J., Hansen T., Bork P., Brunak S., Oresic M., Ehrlich S.D., Pedersen O., Human gut microbes impact host serum metabolome and insulin sensitivity. Nature, 2016, 535(7612), 376–381.

32. Perasso L., Spallarossa P., Gandolfo C., Ruggeri P., Balestrino M., Therapeutic use of creatine in brain or heart ischemia: available data and future perspectives. Med. Res. Rev., 2013, 33(2), 336–363.

33. Ren M., Zhang S.H., Zeng X.F., Liu H., Qiao S.Y., Branched--chain amino acids are beneficial to maintain growth performance and intestinal immune-related function in weaned piglets fed protein restricted diet. Asian-Australas. J. Anim. Sci., 2015, 28(12), 1742–1750.

34. Richards S.E., Wang Y., Claus S.P., Lawler D., Kochhar S., Holmes E., Nicholson J.K., Metabolic phenotype modulation by caloric restriction in a lifelong dog study. J. Proteome Res., 2013, 12(7), 3117–3127.

35. Schoeman J.C., Hou J., Harms A.C., Vreeken R.J., Berger R., Hankemeier T., Boonstra A., Metabolic characterization of the natural progression of chronic hepatitis B. Genome Med., 2016, 8, art. no. 64.

36. Song X., Wang J., Wang P., Tian N., Yang M., Kong L., ^{1}H NMR--based metabolomics approach to evaluate the effect of Xue-Fu-Zhu-Yu decoction on hyperlipidemia rats induced by high-fat diet. J. Pharm. Biomed. Anal., 2013, 78–79, 202–210.

37. Wang X.Y., Luo J.P., Chen R., Zha X.Q., Pan L.H., *Dendrobium huoshanense* polysaccharide prevents ethanol-induced liver injury in mice by metabolomic analysis. Int. J. Biol. Macromol., 2015, 78, 354–362.

38. Wissmann P., Geisler S., Leblhuber F., Fuchs D., Immune activation in patients with Alzheimer's disease is associated with high serum phenylalanine concentrations. J. Neurol. Sci., 2013, 329(1–2), 29–33.

39. Worley B., Halouska S., Powers R., Utilities for quantifying separation in PCA/PLS-DA scores plots. Anal. Biochem., 2013, 433(2), 102–104.

40. Wu B., Yan S., Lin Z., Wang Q., Yang Y., Yang G., Shen Z., Zhang W., Metabolomic study on ageing: NMR-based investiga-tion into rat urinary metabolites and the effect of the total flavone of *Epimedium*. Mol. Biosyst., 2008, 4(8), 855–861.

41. Xia J., Sinelnikov I.V., Han B., Wishart D.S., MetaboAnalyst 3.0—making metabolomics more meaningful, Nucleic Acids Res., 2015, 43, W251-W257.

42. Xu J., Jiang H., Li J., Cheng K.K., Dong J., Chen Z., ^{1}H NMR--based metabolomics investigation of copper-laden rat: a model of Wilson's disease. PLoS One, 2015, 10, art. no. e0119654.

43. Xu X., Yan H., Zhang X., Structure and immuno-stimulating activities of a new heteropolysaccharide from *Lentinula edodes*. J. Agric. Food Chem., 2012, 60(46), 11560–1156.

44. Xu X., Yang J., Luo Z., Zhang X., *Lentinula edodes*-derived poly-saccharide enhances systemic and mucosal immunity by spatial modulation of intestinal gene expression in mice. Food Funct., 2015a, 6(6), 2068–2080.

45. Xu X., Yang J., Ning Z., Zhang X., *Lentinula edodes*-derived polysaccharide rejuvenates mice in terms of immune responses and gut microbiota. Food Funct., 2015b, 6(8), 2653–2663.

46. Xu X., Yang J., Ning Z., Zhang X., Proteomic analysis of intestinal tissues from mice fed with *Lentinula edodes*-derived polysac-charides. Food Funct., 2016, 7(1), 250–261.

47. Xu X., Zhang X., *Lentinula edodes*-derived polysaccharide alters the spatial structure of gut microbiota in mice. PLoS One, 2015, 10(1), art. no. e0115037.

48. Yap I.K., Li J.V., Saric J., Martin F.P., Davies H., Wang Y., Wilson I.D., Nicholson J.K., Utzinger J., Marchesi J.R., Holmes E., Metabonomic and microbiological analysis of the dynamic effect of vancomycin-induced gut microbiota modification in the mouse. J. Proteome Res., 2008, 7(9), 3718–3728.

49. Zhu K.X., Nie S.P., Gong D.M., Xie M.Y., Effect of polysaccha-ride from *Ganoderma atrum* on the serum metabolites of type 2 diabetic rats. Food Hydrocoll., 2016, 53, 31–36.